

Learning to Collocate Visual-Linguistic Neural Modules for Image Captioning

Xu Yang, Hanwang Zhang, Chongyang Gao, Jianfei Cai

Received: date / Accepted: date

Abstract Humans tend to decompose a sentence into different parts like STH DO STH AT SOMEPLACE and then fill each part with certain content. Inspired by this, we follow the *principle of modular design* to propose a novel image captioner: learning to Collocate Visual-Linguistic Neural Modules (CVLMN). Unlike the widely used neural module networks in VQA, where the language (i.e., question) is fully observable, the task of collocating visual-linguistic modules is more challenging. This is because the language is only partially observable, for which we need to dynamically collocate the modules during the process of image captioning. To sum up, we make the following technical contributions to design and train our CVLMN: 1) *distinguishable module design* — four modules in the encoder including one linguistic module for function words and three visual modules for different content words (i.e., noun, adjective, and verb) and another linguistic one in the decoder for commonsense reasoning, 2) a self-attention based *module controller* for robustifying the visual reasoning, 3) a part-of-speech based *syntax loss* imposed on the module controller for further regularizing the training of our CVLMN. Extensive exper-

Xu Yang
 School of Computer Science and Engineering, Southeast University, China,
 E-mail: 101013120@seu.edu.cn

Hanwang Zhang
 School of Computer Science and Engineering, Nanyang Technological University, Singapore,
 E-mail: hanwangzhang@ntu.edu.sg
 He is the corresponding author.

Chongyang Gao
 Computer Science Department, Northwestern University, United States,
 E-mail: cygao@u.northwestern.edu

Jianfei Cai
 Faculty of Information Technology, Monash University, Australia,
 E-mail: Jianfei.Cai@monash.edu

iments on the MS-COCO dataset show that our CVLMN is more effective, e.g., achieving a new state-of-the-art 129.5 CIDEr-D, and more robust, e.g., being less likely to overfit to dataset bias and suffering less when fewer training samples are available. Codes are available at <https://github.com/GCYZSL/CVLMN>.

Keywords Image Captioning · Distinguishable Neural Modules · Soft Module Collocations

1 Introduction

Let us describe the three images in Fig. 1a. Most people will compose sentences varying vastly from image to image. In fact, the ability to use diverse language to describe the colorful visual world is a gift to humans, but a formidable challenge to machines. Although recent advances in visual representation learning [18, 58] and language modeling [20, 69] demonstrate an impressive power of modeling the diversity in their respective modalities, it is still far from establishing a robust cross-modal connection between them.

Actually, most visual reasoning systems tend to overfit to dataset biases and thus fail to reproduce the diversity of our world — the more complex the task is, the severer the overfitting will be, such as VQA [27, 62, 67], image paragraph generation [32], scene graph generation [10], and visual dialog [12, 53]. Similarly, modern image captioning systems also easily exploit dataset bias to generate the captions and sometimes even without looking at the image [60]. For example, in MS-COCO [38] captioning training set, as the co-occurrence frequency of “man” and “standing” is 11% (Fig. 2 (c)), a state-of-the-art captioner [2] is very likely to generate “man standing”, regardless of their actual relationship is “milking”, whose co-occurrence frequency is only 0.023%.

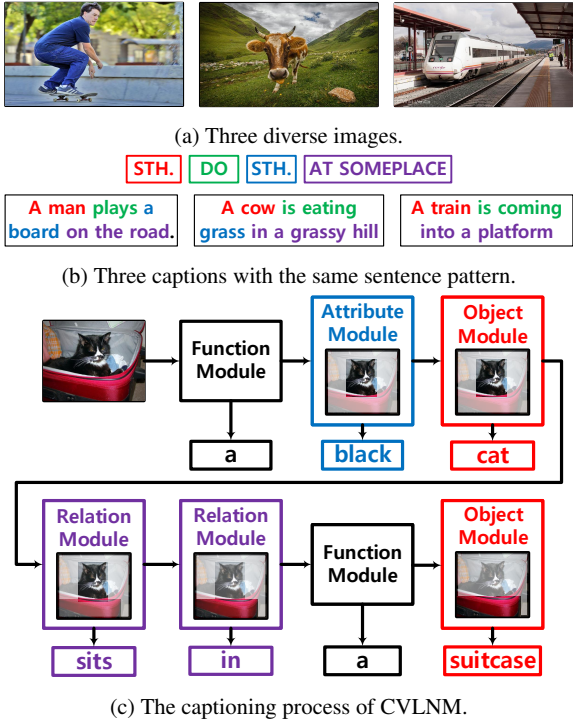


Fig. 1: Motivated by the principle of the modular design, we Collocate Visual-Linguistic Neural Modules (CVLNM) for image captioning.

Unfortunately, unlike a visual concept in ImageNet which has 650 training images on average [13] for image classification, a specific sentence in MS-COCO only corresponds to *one single* image [38], which is extremely scarce in the conventional view of supervised training. However, humans generally do not require many training samples to perform captioning. Since we can decompose a sentence into different parts and then fill suitable contents into each part, e.g., as shown in Figure 1b. Although substantial progress has been made in the past few years since the early work of Vinyals *et al.* [71], such crucial technique has not been well-studied in the field of image captioning.

The missing crux is the *principle of modular design*, which makes a system less likely to overfit to dataset bias since each module only needs to learn its related supervision instead of being entangled by unrelated knowledge [49, 8]. Apart from confronting dataset bias, modular design also enriches the flexibility and extensibility of a learning system that researchers can insert suitable modules for achieving specific goals [4, 21].

Motivated by these advantages, we follow the modular design principle [49, 8] and propose learning to Collocate Visual-Linguistic Neural Modules (CVLNM), which decomposes captioning into a series of sub-tasks that each one is solved by a specific module. To cover the frequently appearing part-of-speech of a sentence, we design an empirical

complete set of modules in the encoder, including OBJECT module for nouns, ATTRIBUTE module for adjectives, RELATION module for verbs, prepositions, and quantifiers, and FUNCTION module for other function words (see Section 3.1). Among them, the former three are visual modules and the last one is a linguistic module. We apply different inductive biases to design these modules and thus they can learn distinguishable information [43] to solve specific sub-tasks, i.e., generate the module-related words. Moreover, our CVLNM is flexible that we can insert other modules for specific goals. In this research, we plug a linguistic REASON module into the decoder to approximate human-like commonsense reasoning for more descriptive captions (see Section 3.4).

Neural module networks have been proposed to solve various vision-language tasks, while most of them parse a module layout from a fully observable sentence, e.g., the question is used to parse a module layout in VQA [4]. However, for image captioning, such fully observable sentences are not available and we only have partially observable sentences during the process of captioning, which increases the difficulty of designing our CVLNM. To address this challenge, we design a multi-head self-attention based module controller to dynamically collocate modules during captioning, conditioned on the visual and linguistic context knowledge (see Section 3.2). With this controller, our CVLNM can discover the frequently appearing syntax patterns from the training dataset and use them to regularize the caption training and generation. During the caption generation, at each time step, we first choose a few modules and then use their outputs to generate the words. Fig. 1c sketches such captioning process where we choose the most responsible module as the example.

Since the module layout is dynamically parsed in image captioning, it is far from perfect compared with the layout in the other visual reasoning tasks where the auxiliary sentences are available [21, 41, 62]. To enhance the effectiveness and robustness of our captioner, the following techniques are also applied. 1) The module controller is designed to softly fuse four distinguishable modules in the encoder to comprehensively exploit their outputs (see Section 3.2.2). 2) A part-of-speech based syntax loss is imposed on the controller to make the generated module layout more faithful to the human-like pattern, e.g., an adjective is usually used before a noun and in such a case the syntax loss will encourage ATTRIBUTE module to be selected before OBJECT module (see Section 3.3). Furthermore, this loss encourages each module to learn its module-specific knowledge for further decomposing the image captioning task.

Extensive discussions and human evaluations are offered in Section 4 to validate the effectiveness and robustness of CVLNM on the challenging MS-COCO image captioning benchmark. Overall, we achieve a new state-of-the-art 129.5

	CVLM: <i>an elephant is standing in a forest</i> Module/O: <i>a elephant is standing in a forest</i> a: 92% an: 8%		CVLM: <i>a herd of sheep grazing on a grassy hill</i> Module/O: <i>a herd of sheep grazing in a field</i> "sheep+grassy hill" / "sheep": 1.3% "sheep+field" / "sheep": 28%		CVLM: <i>a man is milking a cow</i> Module/O: <i>a man is standing next to a cow</i> "man+milking" / "man": 0.023% "man+standing" / "man": 11%
	CVLM: <i>two hot dogs sitting on a plate</i> Module/O: <i>a hot dogs on a plate</i> singular: 68% plural: 32%		CVLM: <i>a dog is wearing a santa hat</i> Module/O: <i>a dog is wearing a hat</i> "dog+santa hat" / "dog": 0.13% "dog+hat" / "dog": 1.9%		CVLM: <i>a red fire hydrant spewing water on a street</i> Module/O: <i>a fire hydrant sitting on a street</i> "hydrant+spewing" / "hydrant": 0.61% "hydrant+sitting" / "hydrant": 14%
(a): Correct Grammar		(b): Descriptive Attributes		(c): Accurate Interactions	

Fig. 2: By comparing our CVLM with the baseline Module/O, which only uses OBJECT module in the encoder (an upgraded version of Up-Down [2]), we have three interesting findings in tackling dataset bias: (a) more accurate grammar, where % in the bottom box for each image denotes the frequency of a certain pattern in MS-COCO, (b) more descriptive attributes, and (c) more accurate object interactions. The ratio ./ denotes the percentage of co-occurrence, e.g., “sheep+field”/“sheep” = 28% means that “sheep” and “field” contributes the 28% occurrences of “sheep”. We can see that CVLM outperforms Module/O even with highly biased training samples.

CIDEr-D score on Karpathy split and 127.8 c40 on the official server. More importantly, by following the principle of modular design, we find that our CVLM is less likely to overfit to dataset bias. For example, compared to a strong non-module baseline Up-Down [2], our CVLM generates 1) more accurate grammar (Fig. 2 (a)) thanks to the joint reasoning of FUNCTION and OBJECT module, 2) more descriptive attributes (Fig. 2 (b)) due to ATTRIBUTE module, and 3) more accurate interactions (Fig. 2 (c)) due to RELATION module. Moreover, we find that when only one training sentence of each image is provided, our CVLM will suffer less performance deterioration compared with the strong non-module baseline. Our contributions can be summarized as:

- Our CVLM is the first module network for image captioning, which is a generic framework with principled module and controller designs. This enriches the spectrum of using neural modules for vision-language tasks.
- We develop an advanced module controller and a syntax based loss for robustifying the dynamic module collocations and meanwhile encouraging each module to learn their module-specific knowledge.
- To show the extensibility of our framework, we plug a REASON module in the decoder to approximate commonsense reasoning for more descriptive captions.
- We conduct extensive experiments with various metrics. Experiment results show the effectiveness and robustness of our CVLM.

This work is an extension of our previous conference paper [77] with significant modifications:

- We refined the module controller with additional inputs from previous module collocations and utilized multi-head self-attention instead of LSTM to generate the current collocation.
- We incorporated a novel REASON module into the decoder to approximate commonsense reasoning for more descriptive captions.

- We carried detailed ablation experiments to demonstrate the effectiveness of these additional refinements.

In addition, we re-organized the introduction, added more details, figures, explanations, results, and analyses. In particular, we analyzed the accuracy of the predicted module layout, the shape of the module distribution, and the module removal effect.

2 Related Work

2.1 Image Captioning

Most early image captioners are template-based models that first generate sentence patterns and then fill the content words like objects’ categories, attributes, and their relations into the fixed patterns [34, 35, 52]. However, since the accuracy of the visual detectors is not satisfactory, and the template generator and the visual detectors are not jointly trained, the performances of these captioners are heavily limited.

Compared with these template-based models, modern captioners which achieve superior performances are most attention based encoder-decoder methods [74, 71, 59, 9, 85, 2, 78, 48, 57, 47]. However, unlike the template-based models, most of the encoder-decoder based models generate word one by one without explicitly exploiting syntax patterns, while various NLP works [29, 66, 61] have proven that syntax patterns provide beneficial inductive bias for improving robustness and effectiveness.

Our CVLM takes advantage from both template and network based captioners, which learns hidden syntax patterns and is trained end-to-end. From the perspective of the module network, several recent captioners can be reduced to special cases of our CVLM. For example, semantic attention based captioners [15, 82] use OBJECT, ATTRIBUTE, and RELATION modules to predict object categories, attributes,

and actions, respectively, and then directly input these semantic words into the language decoder for captioning. However, such captioners do not dynamically collocate these semantic modules and are more like extensions of the traditional attention mechanism. KWL [45], NBT [46], and GCN-LSTM [79] go one step further. They dynamically collocate FUNCTION, OBJECT, and RELATION modules to generate the corresponding words, respectively. Compared to them, our CVLNM designs more fine-grained modules with diverse inductive biases and a more advanced controller for collocating modules. Some captioners also integrate different modules to generate comprehensive embeddings with various semantic knowledge. For example, Up-Down [2] integrates OBJECT and ATTRIBUTE modules by exploiting the object and attribute labels of VG [33] to pre-train a Resnet-101 Faster R-CNN [58] for extracting features; and SGAE [76] applies Graph Neural Network to integrate OBJECT, RELATION, and ATTRIBUTE modules. For HIP [80], it integrates the hierarchical structure of the objects into the visual features. Thus its encoder can be considered as the integration of the object module and the relation module. Although such comprehensive embeddings improve the quality of the generated captions, the interpretability is also lost since we cannot figure out which module contributes more to a specific word. In contrast, our CVLNM can inspect the module fusion weights to identify which module is more responsible for a word.

Some current research papers focus on developing more advanced attention techniques. For example, AoANet [24] designs an Attention on Attention block to capture the relevance between the attention results and the queries. X-LAN [54] applies the X-Linear attention block to model the second-order interactions across multi-modal inputs. Furthermore, some researchers [36, 19, 11, 17] build their captioning models based on the Transformer architecture. For example, ETA [36] integrates semantic and visual knowledge by the multi-head attention as the input features for captioning. Similarly, ToW [19] integrates spatial relations and visual features for captioning. Besides exploiting the relation knowledge between objects, NSA [17] further normalizes self-attention. M^2 -Transformer [11] designs mesh-like connections in the decoder to exploit multi-level visual features.

2.2 Neural Module Networks

For visual reasoning tasks (e.g., image captioning [74] or VQA [5]), they are usually composed by a series of low-level vision tasks (e.g., image classification [63], object detection [18], or relation recognition [44]) and nature language processing tasks (e.g., language generation [65, 69] or language understanding [56, 14]). Then, an intuitive way to solve visual reasoning tasks is to decompose them into

many simple but diverse sub-tasks and design distinguishable modules to address each sub-task.

More specifically, VQA [5] requires an AI agent to understand different aspects of a visual scene and the given question for correctly answering, which can be solved by a series of neural modules [4, 3, 21, 23], e.g., COLOR module for “what is the color of an object”, LOCATE module for “where is one object”, or COUNT module for “how many is one object”. Similarly, visual reasoning [62, 50, 81] and visual grounding [40, 83, 22, 41] can also be decomposed into different sub-tasks addressed by specific modules. In these tasks, high-quality module layouts can be parsed from the provided fully observable sentences like the questions in VQA or the descriptions in visual grounding.

However, in image captioning, only partially observable sentences are available, and thus the module layout cannot be perfectly parsed as other vision-language tasks. To address such a challenge, we design a module controller with the previously generated module layout as input to dynamically collocate neural modules. This controller is also regularized by a part-of-speech based syntax loss for more human-like module layouts.

3 Collocation of Visual-Linguistic Neural Modules

Fig. 3(a) shows the structure of our learning to Collocate Visual-Linguistic Neural Modules (CVLNM) model. The encoder contains a CNN and four neural modules to extract different features (see Section 3.1). Our decoder has a module controller (see Section 3.2) that softly fuses these features into a single feature. This feature is input into a linguistic REASON module for commonsense reasoning (see Section 3.4) and the output is fed into an RNN for language decoding (see Section 3.5). We also impose a part-of-speech based syntax loss on the controller to make it more faithful to human-like syntax patterns and meantime to encourage each module to learn distinguishable knowledge (see Section 3.3).

3.1 Distinguishable Feature Extraction Modules

As sketched in the encoder of Fig. 3(a), we use three visual and one linguistic neural modules to cover the frequently appearing part-of-speech of the captioning dataset, i.e., OBJECT module for nouns; ATTRIBUTE module for adjectives; RELATION module for verbs, prepositions, and quantifiers; and FUNCTION module for other function words. We apply different design principles to encourage these modules to capture different aspects of information about the same image for generating different types of words, making these modules *distinguishable*. For example, the output feature of

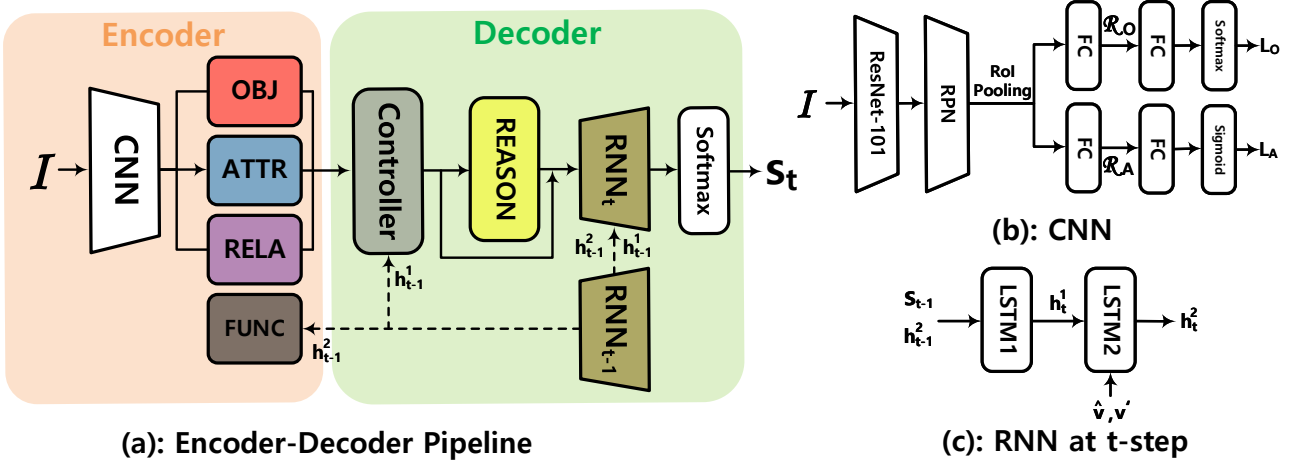


Fig. 3: (a) The encoder-decoder pipeline that Collocates Visual-Linguistic Neural Modules (CVLM) for captioning an input image I . The dash lines from RNN to FUNCTION module and the module controller indicate that both sub-networks require the contextual knowledge of the partially observable sentences, which are the outputs of RNN. The self-loop in RNN denotes the recurrence structure. (b) The deployed CNN is a modified ResNet-101 Faster R-CNN. The top and bottom branches are respectively trained by object and attribute classifications. \mathcal{R}_O and \mathcal{R}_A are the extracted features. (c) The sketch of the Top-Down RNN (Eq. (18)), where s_{t-1} is the last word, and \hat{v}, v' are the outputs of the module controller (Eq. (13)) and REASON module (Eq. (17)).

OBJECT module should be more responsible for generating nouns instead of adjectives.

3.1.1 OBJECT Module

It is a visual module designed to transform the CNN features to a feature set \mathcal{V}_O containing the information about object categories, i.e., \mathcal{V}_O facilitates to generate nouns like “person” or “dog”. The input of this module is the feature set $\mathcal{R}_O \in \mathbb{R}^{N \times d_r}$, where N is the number of detected objects and d_r is the dimension of an ROI feature, whose value is specified in Table 1. \mathcal{R}_O is extracted from the top branch of Fig. 3(b), which is a modified ResNet-101 Faster R-CNN [58]. This branch is pre-trained by object classification using the object annotations of the VG dataset [33]. Specifically, it is pre-trained with the cross-entropy loss:

$$L_O = - \sum_r \log p_{o_r}, \quad (1)$$

where o_r is the object label of the r -th region and p_{o_r} is the predicted probability of the object o_r . In this way, \mathcal{R}_O will contain abundant information about the objects’ categories.

Formally, this module can be written as:

$$\begin{aligned} \text{Input: } & \mathcal{R}_O, \\ \text{Output: } & \mathcal{V}_O = \text{LeakyReLU}(\text{FC}(\mathcal{R}_O)), \end{aligned} \quad (2)$$

where FC denotes the fully-connected layer, LeakyReLU denotes the Leaky ReLU layer [72], $\mathcal{V}_O \in \mathbb{R}^{N \times d_v}$ is the output feature set, and d_v is the feature dimension whose value is specified in Table 1.

3.1.2 ATTRIBUTE Module

It is a visual module designed to transform the CNN features to a feature set \mathcal{V}_A containing attribute information for generating adjectives like “black” or “small”. The input of this module is $\mathcal{R}_A \in \mathbb{R}^{N \times d_r}$, which is extracted from the bottom branch of Fig. 3(b). This branch is pre-trained by multi-label attribute classification using the attribute annotations of VG with the binary cross-entropy loss:

$$L_A = - \sum_r \sum_i a_{r,i} \log p_{a_{r,i}}, \quad (3)$$

where $a_{r,i}$ is a binary variable denoting whether the r -region has the i -th attribute and $p_{a_{r,i}}$ is the predicted possibility of the i -th attribute. After pre-training, \mathcal{R}_A will contain abundant information about objects’ attributes. Formally, this module can be written as:

$$\begin{aligned} \text{Input: } & \mathcal{R}_A, \\ \text{Output: } & \mathcal{V}_A = \text{LeakyReLU}(\text{FC}(\mathcal{R}_A)), \end{aligned} \quad (4)$$

where $\mathcal{V}_A \in \mathbb{R}^{N \times d_v}$ is the output of this module.

3.1.3 RELATION Module

It is a visual module designed to transform CNN features to a feature set \mathcal{V}_R containing information about potential relations between objects, which would help generate verbs like “ride”, prepositions like “on”, or quantifiers like “three”.

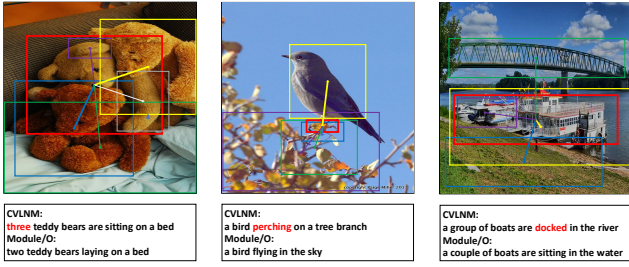


Fig. 4: Three examples show how RELATION module generates relation specific words. The red box is the attended region when RELATION module generates a relation specific word. The thickness of the line connecting two boxes is determined by the soft attention weight computed by Eq. (6), the larger the attention weight, the thicker the line.

This module is built upon the multi-head self-attention mechanism [69], which automatically seeks the relations among the objects during the attention computations between the corresponding features. Here, we use \mathcal{R}_O in Eq. (2) as the input because these kinds of features are widely applied as the inputs for successful relation detections [86, 84]. This module is formulated as:

$$\begin{aligned} \text{Input: } & \mathcal{R}_O, \\ \text{Attention: } & \mathcal{M} = \text{MH-ATT}(\mathcal{R}_O), \\ \text{Output: } & \mathcal{V}_R = \text{LeakyReLU}(\text{MLP}(\mathcal{M})), \end{aligned} \quad (5)$$

where MH-ATT(\cdot) is the multi-head attention mechanism, when the input query, key, and value are the same, it is also called multi-head self-attention; MLP(\cdot) is a feed-forward network containing two fully connected layers with a ReLU activation layer in between [69]: FC-ReLU-FC; and $\mathcal{V}_R \in \mathbb{R}^{N \times d_v}$ is the output of this module. Specifically, the following steps are deployed to compute the MH-ATT. We first use the scaled dot-product to compute k head matrices $\text{head}_i \in \mathbb{R}^{N \times d_k}$:

$$\text{head}_i = \text{Softmax}\left(\frac{\mathcal{R}_O \mathbf{W}_i^1 (\mathcal{R}_O \mathbf{W}_i^2)^T}{\sqrt{d_k}}\right) \mathcal{R}_O \mathbf{W}_i^3, \quad (6)$$

where $\mathbf{W}_i^1, \mathbf{W}_i^2, \mathbf{W}_i^3 \in \mathbb{R}^{d_r \times d_k}$ are all trainable matrices, $d_k = d_r/k$ and k is the number of head matrices. Then these k head matrices are concatenated and linearly projected to the feature set $\mathcal{M} \in \mathbb{R}^{N \times d_r}$:

$$\mathcal{M} = [\text{head}_1, \dots, \text{head}_k] \mathbf{W}_C, \quad (7)$$

where $[\cdot]$ means the concatenation operation and $\mathbf{W}_C \in \mathbb{R}^{d_r \times d_r}$ is a trainable matrix.

Fig. 4 demonstrates how this self-attention based RELATION module generates relation specific words. For example, in the middle figure, at the third time step, RELATION module focuses more on the “paw” part (red box) of the bird, and meantime the clues about “bird” (yellow box) and

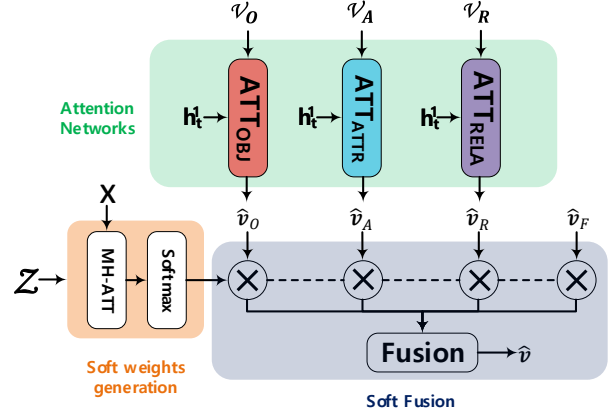


Fig. 5: Our module controller has three matrix-sum attention (MS-ATT) networks (ATT_{OBJ} , ATT_{ATTR} , $\text{ATT}_{\text{RELATION}}$) and a multi-head attention network (MH-ATT). MH-ATT generates four soft weights to fuse the four attended features (\hat{v}_O , \hat{v}_A , \hat{v}_R , \hat{v}_F) into a single feature \hat{v} . h_t^1 (Eq. (9)) is the query vector used in three MS-ATT networks, \mathcal{Z} (Eq. (11)) is the embedding set of the previous module collocations, and x (Eq. (12)) is the query vector used in MH-ATT.

“tree” (blue box) are incorporated to the feature of the “paw” part by MH-ATT. By exhaustively considering these visual clues, a more accurate action “perch” is generated by our RELATION module.

3.1.4 FUNCTION Module

It is a linguistic module designed to produce a single feature \hat{v}_F for generating function words like “a” or “and”. The input of this module is the linguistic context vector $h_t^2 \in \mathbb{R}^{d_h}$ accumulated in the RNN, which is the output of the second LSTM in Fig. 3(c). d_h is the dimension of this context vector, whose value is given in Table 1. We use h_t^2 as the input because it contains rich linguistic context knowledge of the partially generated captions and such knowledge instead of visual knowledge is more beneficial for generating function words. This module is formulated as:

$$\begin{aligned} \text{Input: } & h_t^2, \\ \text{Output: } & \hat{v}_F = \text{LeakyReLU}(\text{FC}(h_t^2)), \end{aligned} \quad (8)$$

where $\hat{v}_F \in \mathbb{R}^{d_v}$ is the output feature.

3.2 Module Controller

It is still an open question on how to define a perfect complete set of neural modules for visual reasoning [83, 4]. We believe that a variety of complex tasks can be approximately accomplished by adaptively selecting modules from an empirically complete module set conditioned on the visual and

linguistic context [23]. Motivated by this, we design a module controller for dynamically collocating the modules when only a partially generated caption is available. Fig. 5 shows the detail of this controller, which contains three matrix-sum attention (MS-ATT) networks and one multi-head attention (MH-ATT) network based soft-weight generator. The fused feature vector \hat{v} is the output of this controller, which will be input into the followed REASON module and RNN for the next step reasoning (Fig. 3). Next, we describe how each component of our module controller works.

3.2.1 Module Attention

Before the soft fusion, three MS-ATT are used to respectively transform three visual modules' output into three more informative features:

$$\begin{aligned} \text{ATT}_{OBJ} : \quad & \hat{v}_O = \text{MS-ATT}(\mathcal{V}_O, \mathbf{h}_t^1), \\ \text{ATT}_{ATTR} : \quad & \hat{v}_A = \text{MS-ATT}(\mathcal{V}_A, \mathbf{h}_t^1), \\ \text{ATT}_{RELA} : \quad & \hat{v}_R = \text{MS-ATT}(\mathcal{V}_R, \mathbf{h}_t^1), \end{aligned} \quad (9)$$

where $\hat{v}_O, \hat{v}_A, \hat{v}_R \in \mathbb{R}^{d_v}$ are the transformed features of $\mathcal{V}_O, \mathcal{V}_A, \mathcal{V}_R$, which are outputs of OBJECT, ATTRIBUTE, RELATION modules (Section 3.1), respectively; $\mathbf{h}_t^1 \in \mathbb{R}^{d_h}$ is the query vector produced by the first LSTM in the RNN as sketched in Fig. 3(c); and three MS-ATT networks own the same structure while the parameters are not shared:

$$\begin{aligned} \text{Input: } & \mathcal{V}, \mathbf{h}, \\ \text{Attention: } & a_i = \omega_a^T \tanh(\mathbf{W}_v \mathbf{v}_i + \mathbf{W}_h \mathbf{h}), \\ & \alpha = \text{softmax}(a), \\ \text{Output: } & \hat{v} = \mathcal{V} \alpha, \end{aligned} \quad (10)$$

where $\mathbf{W}_h \in \mathbb{R}^{d_a \times d_h}, \mathbf{W}_v \in \mathbb{R}^{d_a \times d_v}$ and $\omega_a \in \mathbb{R}^{d_a}$ are all trainable parameters.

3.2.2 Soft Fusion

Since we only have the partially observable caption to parse the module layout, the parsed layout is far from perfect. To enhance the robustness¹, we softly fuse these module outputs to provide more comprehensive vision and language knowledge. After computing the features from each module: $\hat{v}_O, \hat{v}_A, \hat{v}_R$ (Eq. (9)), and \hat{v}_F (Eq. (8)), the controller generates four soft weights to fuse them.

Since the module collocation at each time step is highly related to the previous module collocations, we build this generator upon the MH-ATT network with the previous module collocations \mathcal{Z} as input. We apply MH-ATT instead of LSTM (which is used in our preliminary work [77]) since the current module collocation is possibly related to a more

¹ “Robustness” means that the soft fusion strategy helps generate more “accurate” captions.

remote module collocation and MH-ATT is good at dealing with such long-range dependencies [69, 31].

At time step t , $\mathcal{Z} = \{z_{0:t-1}\} \in \mathbb{R}^{t \times d_z}$ where z_0 is the embedding of the start token and z_t is the embedding of the chosen modules at time step t (Eq. (14)). We first deploy MH-ATT upon \mathcal{Z} to build the connections among collocations in different steps:

$$\hat{\mathcal{Z}} = \text{MH-ATT}(\mathcal{Z}), \quad (11)$$

where MH-ATT(\cdot) has the similar formula as Eq. (6) and (7) with different parameters. Then the multi-modal context vector $\mathbf{x} \in \mathbb{R}^{d_z}$ is used as the query vector to get the current soft collocation weights and \mathbf{x} is:

$$\mathbf{x} = \text{ReLU}(\text{FC}([\hat{v}_O, \hat{v}_A, \hat{v}_R, \mathbf{h}_t^2])), \quad (12)$$

where \mathbf{h}_t^2 is the context vector output by the second LSTM of the RNN as shown in Fig. 3(c). We use \mathbf{x} as the query vector because both the visual clues ($\hat{v}_O, \hat{v}_A, \hat{v}_R$) and the linguistic context (\mathbf{h}_t^2) of the partially generated caption are indispensable for successfully collocating modules. The process of soft fusion is formulated as:

$$\begin{aligned} \text{Input: } & \hat{\mathcal{Z}}, \mathbf{x}, \\ \text{MH-ATT: } & \text{head}_i = \text{Softmax}\left(\frac{\mathbf{x} \mathbf{W}_l^1 (\hat{\mathcal{Z}} \mathbf{W}_l^2)^T}{\sqrt{d_z}}\right) \hat{\mathcal{Z}} \mathbf{W}_l^3, \\ & \hat{\mathbf{x}} = [\text{head}_1, \dots, \text{head}_j] \mathbf{W}_Z, \\ \text{Soft Vector: } & \mathbf{w} = \{w_O, w_A, w_R, w_F\} = \text{Softmax}(\text{FC}(\hat{\mathbf{x}})), \\ \text{Output: } & \hat{v} = [w_O \hat{v}_O, w_A \hat{v}_A, w_R \hat{v}_R, w_F \hat{v}_F], \end{aligned} \quad (13)$$

where $\mathbf{W}_l^1, \mathbf{W}_l^2, \mathbf{W}_l^3 \in \mathbb{R}^{d_z \times d_j}, \mathbf{W}_Z \in \mathbb{R}^{d_z \times d_z}$ are all trainable matrices, $d_j = d_z/j$ is the dimension of each head vector, and j is the number of the head vectors; w_O, w_A, w_R, w_F are scalar fusion weights; and the output fusion vector is $\hat{v} \in \mathbb{R}^{4d_v}$.

After generating the fusion weights \mathbf{w} , we compute the t -th module embedding \mathbf{z}_t as:

$$\mathbf{z}_t = w_O \mathbf{e}_O + w_A \mathbf{e}_A + w_R \mathbf{e}_R + w_F \mathbf{e}_F, \quad (14)$$

where $\mathbf{e}_O, \mathbf{e}_A, \mathbf{e}_R, \mathbf{e}_F \in \mathbb{R}^{d_z}$ are four learnable label embeddings² corresponding to OBJECT, ATTRIBUTE, RELATION, and FUNCTION modules, respectively. The positional encoding [69] is also used to incorporate the position knowledge of the module layout, whose size is set to d_z . This position encoding and \mathbf{z}_t are summed together to get the module embedding, which is used in Eq. (11), while for convenience, we still use \mathbf{z}_t to denote it.

² Learnable label embeddings mean that they are 4-dimensional one hot vectors multiplied with a learnable $4 \times d_z$ matrix.

3.3 Syntax Loss

To further encourage each module to learn distinguishable knowledge, e.g., OBJECT module focuses more on object categories instead of visual attributes, and make the module layout faithful to human-like collocations, e.g., adjectives are usually be said before nouns, we design a part-of-speech based syntax loss and impose it on the module controller.

We build this loss by extracting the words' part-of-speech (e.g., adjectives, nouns, or verbs) from the ground-truth captions by a part-of-speech tagger tool [68]. According to the extracted part-of-speech, we assign each word an one hot vector $\mathbf{w}^* = \{w_O^*, w_A^*, w_R^*, w_F^*\}$, indicating which module should be chosen for generating this word. In particular, we assign OBJECT module to nouns (NN like "bus") by setting $w_O^* = 1$, ATTRIBUTE module to adjectives (ADJ like "green") by setting $w_A^* = 1$; RELATION module to verbs (VB like "drive"), prepositions (PREP like "on"), and quantifiers (CD like "three") by setting $w_R^* = 1$; and FUNCTION module to the other words (CC like "and") by setting $w_F^* = 1$.

Given these expert-guided module tags \mathbf{w}^* , our syntax loss L_s is defined as the cross-entropy value between \mathbf{w}^* and soft fusion weights \mathbf{w} calculated from Eq. (13):

$$L_s = -(w_O^* \log w_O + w_A^* \log w_A + w_R^* \log w_R + w_F^* \log w_F). \quad (15)$$

Importantly, when this loss is imposed on the controller, the soft fusion strategy in Section 3.2.2 approximates to the hard selection that only one module will be responsible for the generated word. For example, when the noun "dog" is the supervision, only $w_O^* = 1$ and w_O in Eq. (13) is encouraged to be 1 due to this syntax loss. Then the \hat{v}_O part in the fusion representation \hat{v} will get more back-propagated gradients from the noun "dog", and thus OBJECT module is more encouraged to learn from this noun. In this way, this syntax loss regularizes the training of the modules to make them more distinguishable. Such argument is validated in Section 4.2 where we find that this loss indeed increases the recall of each module-specific word and the accuracy of the module collocation.

3.4 REASON Module

In addition to distinguishing different aspects of an image during captioning, humans can also achieve commonsense reasoning to summarize or even infer something that is not evidently detected from the image. For example, when we observe some persons holding umbrellas on a wet road, we can infer that it is raining even the raindrops are not obvious (which means OBJECT module can hardly extract evident

information about the object "raindrop"). To equip our captioner with such commonsense reasoning, we plug a linguistic REASON module into the decoder as sketched in Fig. 3(a). This module is inserted between the controller and the RNN to imitate that humans usually achieve commonsense reasoning after grasping the comprehensive knowledge of a visual scene, while such knowledge is preserved in the fused representation \hat{v} (Eq. (13)).

We exploit the ConceptNet [42] dataset, which is built for helping computers to achieve commonsense reasoning, to build our REASON module. We collect the relation triplets from this dataset and embed them into a key-value memory network [64, 51]: $\mathcal{M} = \{\mathbf{m}_1, \mathbf{m}_2, \dots, \mathbf{m}_K\} \in \mathbb{R}^{d_m \times K}$, where each \mathbf{m}_k is the embedding of a relation triplet, which is represented as "subject-predicate-object", e.g., "eagle-type of-bird" or "umbrella-related to-rain". We use an efficient relation embedding operation to get \mathbf{m} :

$$\mathbf{m} = \text{ReLU}(\text{FC}([\mathbf{e}_s, \mathbf{e}_p, \mathbf{e}_o])), \quad (16)$$

where $\mathbf{e}_s, \mathbf{e}_p, \mathbf{e}_o \in \mathbb{R}^{d_e}$ denote trainable word embeddings of the subject, predicate, and object, respectively.

Given this memory network, we apply dot-product attention (DP-ATT) to imitate commonsense reasoning: the fused representation \hat{v} acts as the query and the embedding \mathbf{m}_k acts as both the key and the value:

$$\begin{aligned} \text{Input: } & \hat{v}, \mathcal{M} = \{\mathbf{m}_1, \mathbf{m}_2, \dots, \mathbf{m}_K\} \\ \text{Attention: } & \beta = \text{softmax}(\mathcal{M}^T \mathbf{W}_v \hat{v}), \\ \text{Output: } & \mathbf{v}' = \mathcal{M} \beta = \sum_{k=1}^K \beta_k \mathbf{m}_k, \end{aligned} \quad (17)$$

where $\mathbf{W}_v \in \mathbb{R}^{d_m \times 4d_v}$ is a trainable matrix and \mathbf{v}' is the output of REASON module, which provides commonsense knowledge for the RNN to captioning.

3.5 Training and Inference of CVLNM

As shown in Fig. 3, by using Faster R-CNN [18], five neural modules, the module controller, and Top-Down RNN [2], our CVLNM can predict the probability of the next word s_t given the image \mathcal{I} and the last word s_{t-1} . Specifically, as shown in Fig. 3(c), Top-Down RNN contains two LSTM layers and it generates the word distribution $P(s_t)$ as:

$$\begin{aligned} \text{Input: } & s_{t-1}, \hat{v}, \mathbf{v}' \\ \text{LSTM1: } & \mathbf{h}_t^1 = \text{LSTM1}([\text{Embed}(s_{t-1}), \mathbf{h}_{t-1}^2]) \\ \text{LSTM2: } & \mathbf{h}_t^2 = \text{LSTM2}([\hat{v}, \mathbf{v}', \mathbf{h}_t^1]) \\ \text{Output: } & P(s_t) = \text{Softmax}(\text{FC}(\mathbf{h}_t^2)), \end{aligned} \quad (18)$$

where \hat{v}, \mathbf{v}' are the outputs of the module controller (Eq. (13)) and REASON module (Eq. (17)); $\text{Embed}(\cdot)$ is the learnable word embedding layer; $\text{LSTM1}(\cdot)$ and $\text{LSTM2}(\cdot)$ are two different LSTM layers.

Given the ground-truth caption $\mathcal{S}^* = \{s_{1:T}^*\}$ with part-of-speech tags $\mathcal{W}^* = \{w_{1:T}^*\}$, we can end-to-end train our CVLNM by minimizing the syntax loss L_s defined in Eq. (15) and the language loss L_l . Given the predicted word distribution $P(s)$, we can define the language loss L_l as the cross-entropy loss:

$$L_l = L_{XE} = -\sum_{t=1}^T \log P(s_t^*), \quad (19)$$

or the negative reinforcement learning (RL) based reward [59]:

$$L_l = L_{RL} = -\mathbb{E}_{s_t^* \sim P(s)} [r(s_{1:T}^*; s_{1:T}^*)], \quad (20)$$

where r is a sentence-level metric, e.g., CIDEr-D [70], between the sampled sentence $\mathcal{S}^* = \{s_{1:T}^*\}$ and the ground-truth $\mathcal{S}^* = \{s_{1:T}^*\}$. Then the total loss becomes

$$L = L_l + \lambda L_s, \quad (21)$$

where λ is the weighting of two objectives. During inference, we adopt the beam search strategy [59] with a beam size of 5 to sample the caption from the predicted distribution $P(s)$.

4 Experiments

4.1 Datasets and Settings

MS-COCO [38] has an official split: 82,783/40,504/40,775 images for training/validating/testing, respectively. The 3rd-party Karpathy split [28] provides an off-line test, which has 113,287/5,000/5,000 images for training/validating/testing, respectively. We deployed our models on both splits to validate the effectiveness. The captions were pre-processed by the following steps: the texts were tokenized on white spaces; all the letters were changed to lowercase; the words were removed if they appear less than 5 times and then we had a vocabulary with 10,369 words; each caption was trimmed to a maximum of 16 words.

Visual Genome [33] (VG) is a noisy scene graph dataset that a large number of the object and attribute labels only appear in a few fractions of the whole training annotations. Thus it is a common practice to filter the dataset for better usage. For example, in most scene graph detection models like [73, 75, 84], researchers only use 150 objects and 50 relations to train their scene graph detectors. Researchers in the field of image captioning also filter this dataset, e.g., Up-Down [2] uses a subset with 1600 objects and 400 attributes. Following them, we also filtered this dataset by keeping the labels that appear more than 2,000 times in the training set, which results in 305 objects and 103 attributes remaining. Importantly, since some images co-exist in both VG and

Table 1: The number of trainable parameters.

symbol	equation	number	symbol	equation	number
d_r	Eq. (2)	2048	d_v	Eq. (2)	1000
k	Eq. (6)	8	d_k	Eq. (6)	256
d_h	Eq. (8)	1000	d_a	Eq. (10)	512
d_z	Eq. (13)	1000	j	Eq. (13)	8
d_j	Eq. (13)	125	d_e	Eq. (16)	1000
d_m	Eq. (17)	1000	K	Eq. (17)	10,000

COCO, we filtered out the images and their annotations of VG which appear in the COCO test set. When pre-training the CNN shown in Fig. 3(b), we sequentially minimized L_O (Eq. (1)) and L_A (Eq. (3)) using the object and attribute annotations of VG. After pre-training, we extracted the features as the inputs into different modules.

ConceptNet [42] is a freely-available semantic dataset containing abundant commonsense triplets formed as “subject-predicate-object”. Each triplet is assigned with an important weight. We exploited these weighted triplets to build our REASON module (Section 3.4) for approximating commonsense reasoning. We searched the related triplets from ConceptNet using the words in caption vocabulary as the keys and preserved the top 10,000 searched commonsense triplets into the memory network \mathcal{M} according to the importance weight of each triplet.

Settings. Table 1 summarizes the number of training parameters in each module. We used Adam optimizer [30] to train the whole model. The learning rate was initialized to $5e^{-4}$ and was decayed by 0.8 for every 5 epochs. L_{XE} Eq. (19) and L_{RL} Eq. (20) were in turn used as the language loss to train our CVLNM for 35 epochs and 65 epochs, respectively. In the experiments, we found that the performance is non-sensitive to λ in Eq. (21). By default, we empirically set $\lambda = 1$ and $\lambda = 0.5$ when L_{XE} and L_{RL} were used as the language loss, respectively. The batch size was set to 100.

4.2 Ablation Studies

We conducted extensive ablations to confirm the effectiveness of each component by gradually incorporating them into the pipeline, including four distinguishable modules in the encoder (see Section 3.1), the multi-head attention (MH-ATT) based module controller (see Section 3.2), the part-of-speech based syntax loss (see Section 3.3), and REASON module (see Section 3.4). We arrange the ablation studies by proposing research questions (Q) in Section 4.2.1, specifying miscellaneous metrics in Section 4.2.2, and providing the corresponding empirical answers (A) in Section 4.2.3.

4.2.1 Research Questions and the Corresponding Baselines

Q1: Will each visual feature extraction module introduced in Section 3.1, i.e., OBJECT, ATTRIBUTE, and RELATION modules, learn distinguishable knowledge and then generate more accurate module-specific words, e.g., will OBJECT module generate more accurate nouns? Does CVLNM allow controllable caption generation, e.g., will removing ATTRIBUTE module eliminate all the attribute related words?

To answer them, the following baselines were designed: we only used a single visual module in the encoder to extract features and deployed the Top-Down RNN [2] as the decoder. When OBJECT, ATTRIBUTE, and RELATION modules were used, the baselines are denoted as **Module/O**, **Module/A**, and **Module/R**, respectively. Note that the baseline Module/O is an upgraded version of the Up-Down model [2]. After training the model with all modules, during testing, we cut off a module and then measure the ratio of the corresponding words to all the generated words to inspect the removal effect.

Q2: Will the qualities of the generated captions be improved when the modules in the encoder are fused? How to fuse them to achieve a better performance?

To answer them, the following three strategies were designed, where each one used a specific type of fusion weights. **Col/1** denotes the model which sets all the fusion weights as 1. This is equivalent to using all the module features in the Up-Down model. When learnable soft fusion weights w (Eq. (13)) were used, the method is called **Col/S**. When the Gumbel-Softmax layer [25] was used to transfer w into one hot vector for achieving hard selection, the baseline is called **Col/H**. In both Col/S and Col/H, we input the previous module layout \mathcal{Z} into the MH-ATT based controller to get w .

Q3: Will inputting the previous module layout \mathcal{Z} (Eq. (13)) into the controller generate better soft fusion weights? Will MH-ATT preserve more long-range dependencies between remote module collocations than LSTM (which is deployed in our preliminary work CNM [77])? More importantly, will better soft fusion weights encourage each module to learn its distinguishable knowledge?

To answer them, we compared the following baselines. When we built the controller upon MH-ATT with/without \mathcal{Z} , the baselines are named as **textbf{MH-ATT+Z/MH-ATT}**. In the same vein, when the module controller is built upon LSTM, the baselines are **LSTM+Z/LSTM**. In these baselines, the encoder contains all the four modules, the soft fusion strategy was applied, and we did not use REASON module and the syntax loss. Note that MH-ATT+ \mathcal{Z} equals the baseline Col/S in Q2.

Q4: Will the expert part-of-speech knowledge provided by the syntax loss L_s (Eq. (15)) benefit the model? Will such loss encourage each feature extraction module to learn more distinguishable knowledge?

To answer them, we compared the models by training them with and without L_s . When we used L_s in MH-ATT+ \mathcal{Z} , we have **MH-ATT+Z+L_s**.

Q5: Will REASON module generate more human-like captions?

To answer it, we inserted REASON module into MH-ATT+ \mathcal{Z} to get **MH-ATT+Z+Reason** and compared them.

Q6: Will the integrated model achieve the best performances among all the baselines?

We compared our full **CVLNM** with the other baselines.

Q7: What do the soft weights look like in each step, e.g., are they sharp (putting most weights on one module) or flat? Will each word be generated mostly from a single module or multiple modules?

To answer this, for each word, we computed the average entropy of the module distribution and the average probability of the most responsible module, where “the most responsible” denotes that this module has the largest weight when one word is generated.

Q8: How about changing the hyperparameters, e.g., λ in Eq. (21) and the number of annotations for training our CNN?

We set λ to different fixed values when L_{XE} and L_{RL} were used to train the model, which is named **CVLNM** (λ). We used 1600/400 objects/attributes as Up-Down [2] to pre-train the feature extractor CNN. The model using these features is denoted as **CVLNM+**.

4.2.2 Evaluation Metrics for Answering Questions

To quantitatively answer the above research questions, we applied the following metrics to comprehensively test the effectiveness and robustness of our CVLNM.

1) We measured the similarities between the generated captions and the ground-truth captions by five standard metrics, which are CIDEr-D [70], BLEU [55], METEOR [6], ROUGE [37], and SPICE [1]. CIDEr-D is the most robust one among them. The higher these similarity metrics are, the more human-like the generated captions are.

2) We exploited CHAIRs and CHAIRi [60] to quantitatively measure the bias degree of the generated captions to some objects. The lower CHAIRs and CHAIRi are, the less biased the captions are. Fig. 2 gives some biased examples. Table 2 reports the results on the five similarity metrics and the two bias degree metrics, where the models are trained following the settings in Section 4.1.

3) To confirm whether each feature extraction module learns its module-specific knowledge, we calculated two metrics which are the recall of each module-specific word and the accuracy of the predicted module layout. Here we show how to calculate the recall of the nouns for OBJECT module. For the i -th image, we counted all the non-repetitive nouns from this images’ ground-truth captions and denoted this number as N_{gt}^i . We also counted how many of these

Table 2: The performances of various baselines on Karpathy split. B@4, M, R, C, S, CHs, and CHi denote BLEU@4, METEOR, ROUGE-L, CIDEr-D, SPICE, CHAIRs, and CHAIRi, respectively. The symbols \uparrow and \downarrow mean the higher the better and the lower the better, respectively.

Models	B@4 \uparrow	M \uparrow	R \uparrow	C \uparrow	S \uparrow	CHs \downarrow	CHi \downarrow
Module/O	37.5	27.7	57.5	123.1	21.0	13.8	9.4
Module/A	37.3	27.4	57.1	121.9	20.9	14.3	9.8
Module/R	37.9	27.8	57.8	123.8	21.2	13.6	9.3
Col/1	38.2	27.9	58.1	125.6	21.2	13.5	9.1
Col/H	38.4	28.2	58.3	126.1	21.3	11.7	8.2
Col/S (MH-ATT+ \mathcal{Z})	38.5	28.3	58.4	127.3	21.6	11.3	7.8
LSTM	38.2	28.0	58.2	125.7	21.2	12.4	8.5
LSTM+ \mathcal{Z}	38.4	28.1	58.3	126.3	21.4	12.3	8.4
MH-ATT	38.3	28.0	58.4	126.7	21.2	11.9	8.2
MH-ATT+ \mathcal{Z} +Reason	38.7	28.3	58.6	128.6	21.7	11.0	7.6
MH-ATT+ \mathcal{Z} + L_s	38.9	28.4	58.5	128.4	21.9	10.8	7.4
CVLNM	39.4	28.7	59.1	129.5	22.2	10.5	7.0
CVLNM ($\lambda = 0.1$)	39.1	28.5	59.0	129.2	22.0	10.6	7.1
CVLNM ($\lambda = 1$)	39.4	28.8	59.0	129.4	22.1	10.5	6.9
CVLNM ($\lambda = 5$)	39.1	28.4	58.8	129.2	21.8	10.7	7.1
CVLNM+	39.7	28.9	59.4	130.1	22.4	10.5	6.9

Table 3: The recalls (%) of five part-of-speech words, where nouns correspond to OBJECT module; adjectives correspond to ATTRIBUTE module; and verbs, prepositions, and quantifiers correspond to RELATION module.

Models	nouns	adjectives	verbs	prepositions	quantifiers
Module/A	42.4	12.4	20.2	41.7	14.3
Module/O	44.5	11.5	21.8	42.6	17.1
Module/R	44.3	11.3	22.8	43.5	22.3
LSTM	45.2	13.1	23.1	43.6	23.4
MH-ATT	45.5	13.5	23.4	43.9	24.2
MH-ATT+ \mathcal{Z}	46.3	14.8	23.8	44.2	26.8
MH-ATT+ \mathcal{Z} + L_s	47.6	16.5	24.4	45.1	29.6

nouns non-repetitively appearing in the predicted caption as N_{pre}^i . Then the recall is $\sum_i N_{pre}^i / \sum_i N_{gt}^i$. We reported five different recalls in Table 3: nouns for OBJECT module; adjectives for ATTRIBUTE module; and verbs, prepositions, and quantifiers for RELATION module. To measure the module layout accuracy, for each generated word, we treated the maximum soft fusion weight w (Eq. (13)) as the predicted module and inspected whether it matches with the ground-truth module w^* . We report this accuracy in Table 5.

4) We also invited 20 workers for human evaluation to test the qualities of the generated captions. We exhibited 50 images sampled from the test set to each worker and asked them to pairwise compare the captions generated from three models: Module/O, MH-ATT+ \mathcal{Z} + L_s , and CVLNM. The captions were compared from two aspects: the language aspect that whether the generated captions are fluent and descriptive (the top three pie charts in Fig. 6); and the relevance aspect that whether the generated captions match with the images (the bottom three pie charts).

Table 4: The ratios (%) of different words among all the generated words when cutting off a module, e.g., “-Module/O” means cutting off OBJECT module.

Module	OBJECT	ATTRIBUTE	RELATION	FUNCTION
all modules	54	10	27	9
-Module/O	24	31	34	11
-Module/A	63	1	27	9
-Module/R	62	10	17	11
-Module/F	61	8	30	1

Table 5: The accuracy (%) of the predicted module layout by the module controller. The column “Average” means the average accuracy of all four modules.

Models	OBJECT	ATTRIBUTE	RELATION	FUNCTION	Average
LSTM	56.3	39.7	75.3	27.7	59.4
MH-ATT	62.2	42.3	78.2	29.1	64.2
MH-ATT+ \mathcal{Z}	66.2	46.8	83.8	32.5	68.6
MH-ATT+ \mathcal{Z} + L_s	74.9	55.7	93.0	39.0	77.6

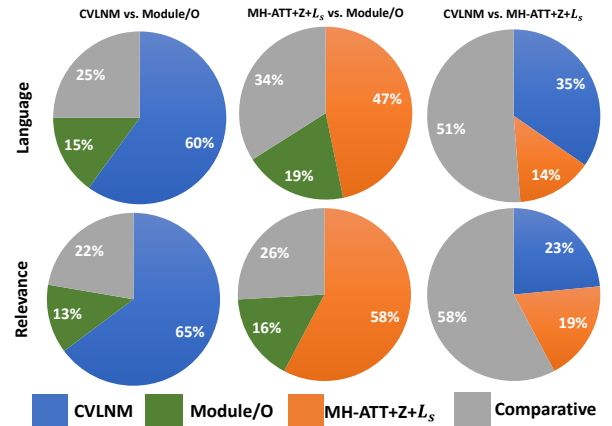


Fig. 6: Each pie chart shows the comparison of two methods in human evaluation.

4.2.3 Empirical Answers

A1: From Table 3, we find that each module prefers to generate more corresponding module-specific words, e.g., among three single-module models, Module/O has the highest recall of nouns. Moreover, in Table 5, we find that even when a simple module controller (the baseline LSTM) is applied to predict the module layout, the accuracy is still much better than randomly choosing (which gives rise to 25% average accuracy)³. Both observations validate that *by using diverse inductive biases to design four modules, they can learn module-specific knowledge to generate more corresponding words and to predict better module layouts*.

³ Intuitively, by randomly choosing, at each time, the probability of choosing the right one from 4 modules is $1/4 = 25\%$.



Fig. 7: Visualizations of the captioning processes Module/O, MH-ATT+ $Z+L_s$, and CVLNM. Different colours refer to different modules, i.e., red/blue/purple/black for OBJECT/ATTRIBUTE/RELATION/FUNCTION module. In Module/O, we use black boxes to show the attended regions. In the other two methods, for simplicity, we only show the module with the largest soft module collocation weight (Eq. (13)) and the corresponding region with the largest attention weight (Eq. (10)). In CVLNM, the number in the bracket is the corresponding soft module weight.

From Table 4, we can find that when one module is cut off, the ratio of the corresponding word will largely decrease, e.g., after cutting off ATTRIBUTE module, ATTRIBUTE related words will decrease from 10% to 1%. However, these words will not be eliminated. The major reason is that the other modules and the language decoder (two LSTM layers in Eq. (18)) will leak certain attribute related information for generating attributes.

A2: As shown in Table 2, when we fuse the modules by three different strategies, the performances are all improved compared with the single-module baselines, e.g., Col/1 is better than Module/R, which answers the first part of Q2 that *fusing modules will generate better captions*.

To answer the second part of Q2, we first observe that in Table 2, both the hard selection (Col/H) and the soft fusion (Col/S) achieve better performances than equally exploiting

the modules (Col/1), which suggests that *the modules should be discriminatively fused*. Furthermore, we find that Col/S outperforms Col/H. One possible reason is that the module layout is parsed from the partially generated caption, which is not perfect enough and the complement of the other modules is necessary.

A3: In Table 2, 3 and 5, we can find that when MH-ATT is applied (MH-ATT vs. LSTM) and when \mathcal{Z} is used (MH-ATT+ \mathcal{Z} vs. MH-ATT), the similarity scores, the recalls, and the layout accuracies are all improved. All of these observations confirm that compared with the module controller in our preliminary work [77], which corresponds to the baseline LSTM, *applying MH-ATT and inputting \mathcal{Z} will enhance the effectiveness of the module controller, which then gives rise to more distinguishable modules and better captions*.

A4: By comparing MH-ATT+ \mathcal{Z} + L_s with MH-ATT+ \mathcal{Z} in Tables 2, 3, and 5, we find that MH-ATT+ \mathcal{Z} + L_s achieves better results. Specifically, the improvements of the word recall and the module accuracy validate that *the syntax loss encourages each module to learn more distinguishable knowledge*, and higher CIDEr scores and lower bias metrics suggest that *more distinguishable modules lead to more human-like and less biased captions*.

A5: In Table 2 and Fig 6, we respectively observe that when REASON module is applied, the similarity scores are improved (MH-ATT+ \mathcal{Z} +REASON vs. MH-ATT+ \mathcal{Z}) and the captions are considered better by humans (CVLNM vs. MH-ATT+ \mathcal{Z} + L_s), especially in terms of language descriptive-ness. Both comparisons suggest that REASON module improves the quality of the generated captions by approximating human-like commonsense reasoning. Also, as shown in Figure 7 (a), we observe that in CVLNM, the word “rain” is generated by the region covering “umbrella” and “wet floor”, while when REASON module is not used, the word “rain” is not generated in MH-ATT+ \mathcal{Z} + L_s .

A6: In Tables 2, 3, 5 and Fig. 6, we find that by sequentially incorporating the module controller, the syntax loss, and REASON module into the pipeline, more distinguishable modules can be learned, lower bias degree can be achieved, and better captions can be generated. Fig. 7 gives two examples to show how CVLNM collocates the modules to generate the captions, which also demonstrates that our CVLNM has better interpretability than the single module based captioner.

A7: Figure 8 shows the average entropy and the average probability for each word. It can be found that for most words, the entropy is small and the probability is large, e.g., a large number of words have a probability larger than 0.8, which indicates that the module distributions are sharp in most cases. Figure 7 also gives two examples, where we can see that most words are generated mainly from one module.

A8: The bottom part of Table 2 shows the results of using different hyperparameters. It can be observed that using dif-

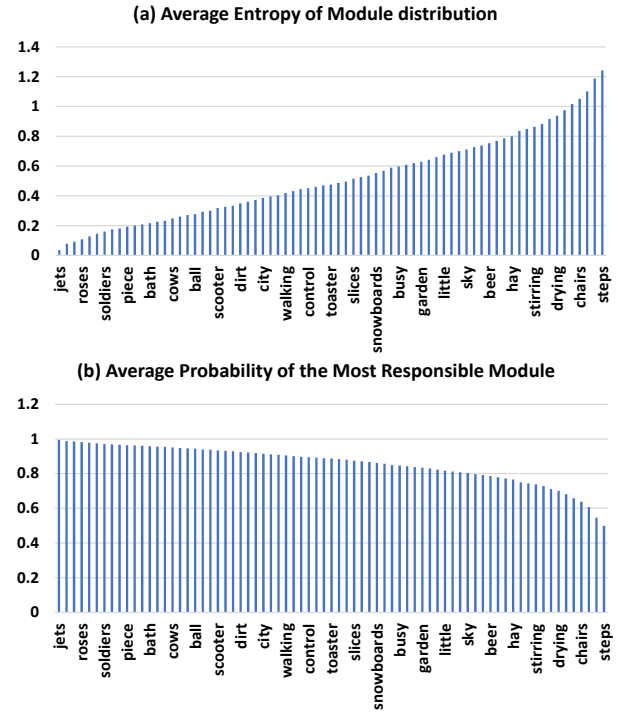


Fig. 8: The average entropy of the module distribution and the average probability of the most responsible module for each word.

ferent λ does not largely affect the performances, e.g., when setting $\lambda = 5$, CIDEr-D only changes 0.3 compared with the original CVLNM. Also, by using more object and attribute annotations to pre-train the CNN for extracting features, the performances have certain improvements, e.g., the CIDEr-D increases from 129.5 (CVLNM) to 130.1 (CVLNM+).

4.3 Comparisons with the State-of-The-Art Models

Comparing Methods. We compared CVLNM with the following state-of-the-art image captioners: **SCST** [59], **Up-Down** [2], **NBT** [46], **CAVP** [85], **RFNet** [26], **LBPF** [57], **GCN-LSTM** [79], **SGAE** [76], **HIP** [80], **ETA** [36], **ToW** [19] and **AoANet** [24]. Some of them can be treated as simple versions of our CVLNM, e.g., NBT only uses OBJECT module, CAVP and GCN-LSTM apply different RELATION modules, and Up-Down integrates OBJECT and ATTRIBUTE modules. RFNet uses various CNN architectures to extract visual features, which owns a wider encoder compared with some other methods, and its comparison with our CVLNM is to prove that only a wider encoder is not enough for better captions. SGAE not only exploits the additional scene graph annotations but also uses Graph Neural Network (GNN) to embed such visual scene graphs to transfer linguistic inductive bias from the pure language domain to the vision-

Table 6: The performances of various methods on MS-COCO Karpathy split trained by cross-entropy loss only (left part) and the mixture of cross-entropy loss and self-critical reward (right part).

Loss Models	Cross-Entropy					Cross-Entropy & Self-Critical				
	B@4	M	R	C	S	B@4	M	R	C	S
SCST [59]	30.0	25.9	53.4	99.4	—	34.2	26.7	55.7	114.0	—
StackCap [16]	35.2	26.5	—	109.1	—	36.1	27.4	—	120.4	—
NBT [46]	34.7	27.1	—	108.9	20.1	—	—	—	—	—
Up-Down [2]	36.2	27.0	56.4	113.5	20.3	36.3	27.7	56.9	120.1	21.4
RFNet [26]	37.0	27.9	57.3	116.3	20.8	37.9	28.3	58.3	125.7	21.7
GCN-LSTM [79]	36.8	27.9	57.0	116.3	20.9	38.2	28.5	58.3	127.6	22.0
CAVP [85]	—	—	—	—	—	38.6	28.3	58.5	126.3	21.6
LBPF [57]	37.4	28.1	57.5	116.4	21.2	38.3	28.5	58.4	127.6	22.0
SGAE [76]	36.9	27.7	57.2	116.7	20.9	38.4	28.4	58.6	127.8	22.1
CNM [77]	37.1	27.9	57.3	116.6	20.8	38.9	28.4	58.8	127.9	22.0
HIP+Up-Down [80]	37.0	28.1	57.1	116.6	21.2	38.2	28.4	58.3	127.2	21.9
HIP+GCN-LSTM [80]	38.0	28.6	57.8	120.3	21.4	39.1	28.9	59.2	130.6	22.3
ETA [36]	37.1	28.2	57.1	117.9	21.4	39.3	28.8	58.9	126.6	22.7
ToW [19]	35.5	28.0	56.6	115.3	21.2	38.6	28.7	58.4	128.3	22.6
CVLNM	37.3	28.2	57.6	117.1	21.2	39.4	28.7	59.1	129.5	22.2
AoANet [24]	37.2	28.4	57.5	119.8	21.3	38.9	29.2	58.8	129.8	22.4
CVLNM*	37.4	28.3	57.8	119.2	21.3	39.6	29.1	59.4	130.2	22.5

Table 7: The performances of various compared image captioners on the online MS-COCO test server.

Model Metric	B@3		B@4		M		R-L		C-D	
	c5	c40	c5	c40	c5	c40	c5	c40	c5	c40
SCST [59]	47.0	75.9	35.2	64.5	27.0	35.5	56.3	70.7	114.7	116.0
LSTM-A [78]	47.6	76.5	35.6	65.2	27.0	35.4	56.4	70.5	116.0	118.0
StackCap [16]	46.8	76.0	34.9	64.6	27.0	35.6	56.2	70.6	114.8	118.3
Up-Down [2]	49.1	79.4	36.9	68.5	27.6	36.7	57.1	72.4	117.9	120.5
RFNet [26]	50.1	80.4	38.0	69.2	28.2	37.2	58.2	73.1	122.9	125.1
CAVP [39]	50.0	79.7	37.9	69.0	28.1	37.0	58.2	73.1	121.6	123.8
SGAE [76]	50.1	79.6	37.8	68.7	28.1	37.0	58.2	73.1	122.7	125.5
CNM [77]	50.2	79.8	38.4	69.3	28.2	37.2	58.4	73.4	123.8	126.0
AoANet [24]	51.4	81.3	39.4	71.2	29.1	38.5	58.9	74.5	126.9	129.6
HIP+GCN-LSTM [80]	51.5	81.6	39.3	71.0	28.8	38.1	59.0	74.1	127.9	130.2
ETA [36]	50.9	80.4	38.9	70.2	28.6	38.0	58.6	73.9	122.1	124.4
CVLNM	50.5	80.4	38.5	70.0	28.7	38.0	58.5	73.7	125.2	127.8
CVLNM-Ensemble	51.2	81.2	39.1	70.9	28.8	38.2	58.8	74.2	126.6	129.1

Table 8: The CIDEr-D deterioration (the difference of scores) of using fewer training sentences. The values in the bracket are the real CIDEr-D scores.

X	5	4	3	2	1
Module-O&X	0(123.1)	0.9(122.2)	2.3(120.8)	4.1(119.0)	6.8(116.3)
MH-ATT+Z&X	0(127.1)	0.5(126.6)	1.4(125.7)	3.0(124.1)	4.5(122.6)
MH-ATT+Z+L _s &X	0(128.4)	0.3 (128.1)	1.0 (127.4)	2.1 (126.3)	3.6 (124.8)

language domain for more descriptive captions. In CVLNM, REASON module has a similar function which transfers linguistic inductive bias. Moreover, we compared our CVLNM with our previous CNM [77] to show that by a more advanced module controller and REASON module, better captions can be generated.

For AoANet, it uses four stronger techniques compared with our CVLNM. First, their Attention on Attention (AoA) is indeed a more effective attention mechanism than the one

(Eq. (10)) used in our CVLNM, which comes from the classic Top-Down attention [2]. Second, AoANet stacks 6 AoA layers as their encoder, which is more similar to the architecture of Transformer [69] instead of the classic Top-Down RNN. Third, AoANet uses a better strategy to adjust the learning rate. In particular, they anneal the learning rate by 0.5 when the CIDEr-D score on the validation split does not improve. Fourth, AoANet uses scheduled sampling [7] when the cross-entropy loss is used to train their network, which can largely improve the CIDEr-D score. Since the latter two general techniques can be used in any captioner, we also applied them to train a model named CVLNM*. Specifically, when the CIDEr-D score on the validation split did not improve for 3 epochs, we annealed the learning rate by 0.5. We also increased the scheduled sampling probability from 0 at the beginning by 0.05 every 5 epochs as AoANet when the cross-entropy loss was used.

Results and Analysis. The left and right parts of Table 6 report the performances of various methods trained by cross-entropy loss and the mixture of cross-entropy loss and self-critical reward, respectively. From both parts, we can see that CVLNM outperforms the other Top-Down RNN based models and it achieves a new state-of-the-art 129.5 CIDEr-D score when the mixture training losses are applied. Specifically, by using four distinguishable feature extraction modules, an advanced module controller, the syntax loss, and REASON module, our CVLNM significantly outperforms the single-module models, e.g., NBT, CAVP, and GCN-LSTM; the model with a wider encoder, e.g., RFNet; and the GNN based model, e.g., SGAE. Due to the more advanced module controller and REASON module, CVLNM outperforms CNM. Compared with AoANet, after using the two advanced training strategies as them, our CVLNM* can achieve comparable performances. When only the cross-entropy loss is used, AoANet’s CIDEr-D is slightly better; when the mixture losses are used, our CVLNM* obtains a slightly higher CIDEr-D score. Since HIP [80] applies more fine-grained segmentation annotations, the extracted visual features are better than our features trained by detection. However, we still achieve better performances than HIP+Up-Down and comparable performances with HIP+GCN-LSTM (which uses GCN [79] as the encoder to further improve the captioning model). Both ETA [36] and ToW [19] use Transformer as the backbone while our CVLNM uses more traditional LSTM-based architecture and still outperforms them. Such comparisons also confirm the validness of our model.

Moreover, we submitted our CVLNM to the online server and report the scores in Table 7, where CVLNM denotes the single-model and CVLNM-Ensemble denotes the ensemble models (We follow the previous researchers [2, 24, 26] to ensemble 4 models.). In the online testing, HIP+GCN-LSTM utilizes SENet-154 as the backbone of Faster R-CNN and Mask R-CNN (while we use ResNet as the backbone of Faster R-CNN and does not use Mask R-CNN) to extract the visual features and thus achieves the best performances. For AoANet, which uses four stronger strategies to train their models, our CVLNM-Ensemble can still achieve comparable results. When compared with the other models like ETA [36] and ToW [19], our models can outperform them.

4.4 Few-Shot Image Captioning

Comparing Methods. In this setting, for each image, we randomly sampled X captions from 5 ground-truth captions to train our models. To avoid confusion with the methods in Section 4.2, we add **&X** to each method to denote that only X captions were provided, e.g., **Module-O&2** means 2 captions of each image were sampled to train Module-O. We compared the following baselines to see how each

component affects the robustness: 1) **Module-O&X** to test only one module, 2) **MH-ATT+Z&X** to test the soft fusion, and 3) **MH-ATT+Z+L_s&X** to test the syntax loss. Noteworthy, for fair comparisons with Module-O&X, we did not pre-train ATTRIBUTE module with attribute labels and did not use REASON module in MH-ATT+Z&X and MH-ATT+Z+L_s&X. The results are reported in Table 8, where the values in the table are the deterioration of CIDEr-D scores compared with the model trained by all 5 sentences, whose scores are given in the bracket.

Results and Analysis. From Table 8, we can find that all the models achieve lower performances when fewer training sentences are provided. Interestingly, we observe that our MH-ATT+Z+L_s&X can almost halve the CIDEr-D deterioration compared to Module/O&X. For example, when only 1 caption is available, the deterioration of MH-ATT+Z+L_s is 3.6, while Module-O is 6.8. Also, it can be found that when we apply the soft fusion strategy and impose the syntax loss to further regularize the learning, the deterioration caused by fewer training samples becomes less severe. Such observations suggest that *by decomposing the captioning into a series of sub-tasks solved by distinguishable modules and by applying suitable fusion and learning strategies, the whole system becomes more robust.*

5 Conclusions

We proposed to follow the principle of modular design for image captioning. In particular, we presented a novel module network: learning to Collocate Visual-Linguistic Neural Modules (CVLNM), which can generate captions by filling the contents into the collocated patterns. In CVLNM, we designed four modules with diverse inductive biases in the encoder to extract features and one REASON module in the decoder to approximate commonsense reasoning. A multi-head self-attention based module controller was designed to dynamically collocate the feature extraction modules since only the partially observable caption is available. A syntax based loss was imposed on the module controller to further guarantee each feature extraction module to learn module-specific knowledge as well as encouraging the controller to learn human-like sentence patterns. We validated the effectiveness and robustness of our CVLNM by extensive ablations and comparisons with the state-of-the-art models on MS-COCO. The experiment results substantially demonstrated that our CVLNM not only generates more human-like captions but also suffers less deterioration when fewer captions are provided for training.

References

- Anderson P, Fernando B, Johnson M, Gould S (2016) Spice: Semantic propositional image caption evaluation. In: European Conference on Computer Vision, Springer, pp 382–398 [10](#)
- Anderson P, He X, Buehler C, Teney D, Johnson M, Gould S, Zhang L (2018) Bottom-up and top-down attention for image captioning and visual question answering. In: CVPR, 5, p 6 [1, 3, 4, 8, 9, 10, 13, 14, 15](#)
- Andreas J, Rohrbach M, Darrell T, Klein D (2016) Learning to compose neural networks for question answering. In: Proceedings of NAACL-HLT, pp 1545–1554 [4](#)
- Andreas J, Rohrbach M, Darrell T, Klein D (2016) Neural module networks. In: Proceedings of the IEEE Conference on Computer Vision and Pattern Recognition, pp 39–48 [2, 4, 6](#)
- Antol S, Agrawal A, Lu J, Mitchell M, Batra D, Lawrence Zitnick C, Parikh D (2015) Vqa: Visual question answering. In: Proceedings of the IEEE international conference on computer vision, pp 2425–2433 [4](#)
- Banerjee S, Lavie A (2005) Meteor: An automatic metric for mt evaluation with improved correlation with human judgments. In: Proceedings of the acl workshop on intrinsic and extrinsic evaluation measures for machine translation and/or summarization, pp 65–72 [10](#)
- Bengio S, Vinyals O, Jaitly N, Shazeer N (2015) Scheduled sampling for sequence prediction with recurrent neural networks. Advances in Neural Information Processing Systems 28: Annual Conference on Neural Information Processing Systems [14](#)
- Bengio Y, Courville A, Vincent P (2013) Representation learning: A review and new perspectives. IEEE transactions on pattern analysis and machine intelligence 35(8):1798–1828 [2](#)
- Chen L, Zhang H, Xiao J, Nie L, Shao J, Liu W, Chua TS (2017) Sca-cnn: Spatial and channel-wise attention in convolutional networks for image captioning. In: CVPR [3](#)
- Chen L, Zhang H, Xiao J, He X, Pu S, Chang SF (2019) Counterfactual critic multi-agent training for scene graph generation. In: ICCV [1](#)
- Cornia M, Stefanini M, Baraldi L, Cucchiara R (2020) Meshed-memory transformer for image captioning. In: Proceedings of the IEEE/CVF Conference on Computer Vision and Pattern Recognition, pp 10578–10587 [4](#)
- Das A, Kottur S, Gupta K, Singh A, Yadav D, Moura JM, Parikh D, Batra D (2017) Visual dialog. In: Proceedings of the IEEE Conference on Computer Vision and Pattern Recognition, pp 326–335 [1](#)
- Deng J, Dong W, Socher R, Li LJ, Li K, Fei-Fei L (2009) Imagenet: A large-scale hierarchical image database. In: 2009 IEEE conference on computer vision and pattern recognition, Ieee, pp 248–255 [2](#)
- Devlin J, Chang MW, Lee K, Toutanova K (2019) Bert: Pre-training of deep bidirectional transformers for language understanding. NAACL-HLT [4](#)
- Gan Z, Gan C, He X, Pu Y, Tran K, Gao J, Carin L, Deng L (2017) Semantic compositional networks for visual captioning. In: Proceedings of the IEEE conference on computer vision and pattern recognition, pp 5630–5639 [3](#)
- Gu J, Cai J, Wang G, Chen T (2017) Stack-captioning: Coarse-to-fine learning for image captioning. AAAI [14](#)
- Guo L, Liu J, Zhu X, Yao P, Lu S, Lu H (2020) Normalized and geometry-aware self-attention network for image captioning. In: Proceedings of the IEEE/CVF Conference on Computer Vision and Pattern Recognition, pp 10327–10336 [4](#)
- He K, Zhang X, Ren S, Sun J (2016) Deep residual learning for image recognition. In: Proceedings of the IEEE conference on computer vision and pattern recognition, pp 770–778 [1, 4, 8](#)
- Herdade S, Kappeler A, Boakye K, Soares J (2019) Image captioning: Transforming objects into words. Advances in Neural Information Processing Systems 32:11137–11147 [4, 13, 14, 15](#)
- Hochreiter S, Schmidhuber J (1997) Long short-term memory. Neural computation 9(8):1735–1780 [1](#)
- Hu R, Andreas J, Rohrbach M, Darrell T, Saenko K (2017) Learning to reason: End-to-end module networks for visual question answering. In: Proceedings of the IEEE International Conference on Computer Vision, pp 804–813 [2, 4](#)
- Hu R, Rohrbach M, Andreas J, Darrell T, Saenko K (2017) Modeling relationships in referential expressions with compositional modular networks. In: Proceedings of the IEEE Conference on Computer Vision and Pattern Recognition, pp 1115–1124 [4](#)
- Hu R, Andreas J, Darrell T, Saenko K (2018) Explainable neural computation via stack neural module networks. In: Proceedings of the European Conference on Computer Vision (ECCV), pp 53–69 [4, 7](#)
- Huang L, Wang W, Chen J, Wei XY (2019) Attention on attention for image captioning. In: Proceedings of the IEEE/CVF International Conference on Computer Vision, pp 4634–4643 [4, 13, 14, 15](#)
- Jang E, Gu S, Poole B (2017) Categorical reparameterization with gumbel-softmax. 5th International Conference on Learning Representations [10](#)
- Jiang W, Ma L, Jiang YG, Liu W, Zhang T (2018) Recurrent fusion network for image captioning. In: Proceedings of the European Conference on Computer Vi-

sion (ECCV), pp 499–515 13, 14, 15

27. Johnson J, Hariharan B, van der Maaten L, Fei-Fei L, Lawrence Zitnick C, Girshick R (2017) Clevr: A diagnostic dataset for compositional language and elementary visual reasoning. In: Proceedings of the IEEE Conference on Computer Vision and Pattern Recognition, pp 2901–2910 1

28. Karpathy A, Fei-Fei L (2015) Deep visual-semantic alignments for generating image descriptions. In: Proceedings of the IEEE conference on computer vision and pattern recognition, pp 3128–3137 9

29. Kim Y, Denton C, Hoang L, Rush AM (2017) Structured attention networks. 5th International Conference on Learning Representations 3

30. Kingma DP, Ba J (2015) Adam: A method for stochastic optimization. 3rd International Conference on Learning Representations 9

31. Kitaev N, Klein D (2018) Constituency parsing with a self-attentive encoder. Proceedings of the 56th Annual Meeting of the Association for Computational Linguistics 7

32. Krause J, Johnson J, Krishna R, Fei-Fei L (2017) A hierarchical approach for generating descriptive image paragraphs. In: Proceedings of the IEEE Conference on Computer Vision and Pattern Recognition, pp 317–325 1

33. Krishna R, Zhu Y, Groth O, Johnson J, Hata K, Kravitz J, Chen S, Kalantidis Y, Li LJ, Shamma DA, et al. (2017) Visual genome: Connecting language and vision using crowdsourced dense image annotations. International Journal of Computer Vision 123(1):32–73 4, 5, 9

34. Kulkarni G, Premraj V, Dhar S, Li S, Choi Y, Berg AC, Berg TL (2011) Baby talk: Understanding and generating image descriptions. In: Proceedings of the 24th CVPR, Citeseer 3

35. Kuznetsova P, Ordonez V, Berg AC, Berg TL, Choi Y (2012) Collective generation of natural image descriptions. In: Proceedings of the 50th Annual Meeting of the Association for Computational Linguistics: Long Papers-Volume 1, Association for Computational Linguistics, pp 359–368 3

36. Li G, Zhu L, Liu P, Yang Y (2019) Entangled transformer for image captioning. In: Proceedings of the IEEE/CVF International Conference on Computer Vision, pp 8928–8937 4, 13, 14, 15

37. Lin CY (2004) Rouge: A package for automatic evaluation of summaries. Text Summarization Branches Out 10

38. Lin TY, Maire M, Belongie S, Hays J, Perona P, Ramanan D, Dollár P, Zitnick CL (2014) Microsoft coco: Common objects in context. In: European conference on computer vision, Springer, pp 740–755 1, 2, 9

39. Liu D, Zha ZJ, Zhang H, Zhang Y, Wu F (2018) Context-aware visual policy network for sequence-level image captioning. In: Proceedings of the 26th ACM international conference on Multimedia, pp 1416–1424 14

40. Liu D, Zhang H, Zha ZJ, Wu F (2018) Explainability by parsing: Neural module tree networks for natural language visual grounding. arXiv preprint arXiv:181203299 4

41. Liu D, Zhang H, Wu F, Zha ZJ (2019) Learning to assemble neural module tree networks for visual grounding. In: Proceedings of the IEEE International Conference on Computer Vision, pp 4673–4682 2, 4

42. Liu H, Singh P (2004) Conceptnet—a practical commonsense reasoning tool-kit. BT technology journal 22(4):211–226 8, 9

43. Locatello F, Bauer S, Lucic M, Rätsch G, Gelly S, Schölkopf B, Bachem O (2019) Challenging common assumptions in the unsupervised learning of disentangled representations. Proceedings of the 36th International Conference on Machine Learning 2

44. Lu C, Krishna R, Bernstein M, Fei-Fei L (2016) Visual relationship detection with language priors. In: European conference on computer vision, Springer, pp 852–869 4

45. Lu J, Xiong C, Parikh D, Socher R (2017) Knowing when to look: Adaptive attention via a visual sentinel for image captioning. In: Proceedings of the IEEE Conference on Computer Vision and Pattern Recognition (CVPR), vol 6, p 2 4

46. Lu J, Yang J, Batra D, Parikh D (2018) Neural baby talk. In: Proceedings of the IEEE Conference on Computer Vision and Pattern Recognition, pp 7219–7228 4, 13, 14

47. Luo R (2017) An image captioning codebase in pytorch 3

48. Luo R, Price B, Cohen S, Shakhnarovich G (2018) Discriminability objective for training descriptive captions. In: Proceedings of the IEEE Conference on Computer Vision and Pattern Recognition, pp 6964–6974 3

49. Marr D (1982) Vision: A Computational Investigation into the Human Representation and Processing of Visual Information. Henry Holt and Co., Inc., New York, NY, USA 2

50. Mascharka D, Tran P, Soklaski R, Majumdar A (2018) Transparency by design: Closing the gap between performance and interpretability in visual reasoning. In: Proceedings of the IEEE conference on computer vision and pattern recognition, pp 4942–4950 4

51. Miller A, Fisch A, Dodge J, Karimi AH, Bordes A, Weston J (2016) Key-value memory networks for directly reading documents. Proceedings of the 2016 Conference on Empirical Methods in Natural Language Pro-

cessing 8

52. Mitchell M, Han X, Dodge J, Mensch A, Goyal A, Berg A, Yamaguchi K, Berg T, Stratos K, Daumé III H (2012) Midge: Generating image descriptions from computer vision detections. In: Proceedings of the 13th Conference of the European Chapter of the Association for Computational Linguistics, Association for Computational Linguistics, pp 747–756 3

53. Niu Y, Zhang H, Zhang M, Zhang J, Lu Z, Wen JR (2019) Recursive visual attention in visual dialog. In: The IEEE Conference on Computer Vision and Pattern Recognition (CVPR) 1

54. Pan Y, Yao T, Li Y, Mei T (2020) X-linear attention networks for image captioning. In: Proceedings of the IEEE/CVF Conference on Computer Vision and Pattern Recognition, pp 10971–10980 4

55. Papineni K, Roukos S, Ward T, Zhu WJ (2002) Bleu: a method for automatic evaluation of machine translation. In: Proceedings of the 40th annual meeting on association for computational linguistics, Association for Computational Linguistics, pp 311–318 10

56. Peters ME, Neumann M, Iyyer M, Gardner M, Clark C, Lee K, Zettlemoyer L (2018) Deep contextualized word representations. Proceedings of the 2018 Conference of the North American Chapter of the Association for Computational Linguistics: Human Language Technologies 4

57. Qin Y, Du J, Zhang Y, Lu H (2019) Look back and predict forward in image captioning. In: Proceedings of the IEEE Conference on Computer Vision and Pattern Recognition, pp 8367–8375 3, 13, 14

58. Ren S, He K, Girshick R, Sun J (2015) Faster r-cnn: Towards real-time object detection with region proposal networks. In: Advances in neural information processing systems, pp 91–99 1, 4, 5

59. Rennie SJ, Marcheret E, Mroueh Y, Ross J, Goel V (2017) Self-critical sequence training for image captioning. In: CVPR, vol 1, p 3 3, 9, 13, 14

60. Rohrbach A, Hendricks LA, Burns K, Darrell T, Saenko K (2018) Object hallucination in image captioning. Proceedings of the 2018 Conference on Empirical Methods in Natural Language Processing 1, 10

61. Shen Y, Tan S, Sordoni A, Courville A (2019) Ordered neurons: Integrating tree structures into recurrent neural networks. 7th International Conference on Learning Representations 3

62. Shi J, Zhang H, Li J (2019) Explainable and explicit visual reasoning over scene graphs. In: Proceedings of the IEEE/CVF Conference on Computer Vision and Pattern Recognition, pp 8376–8384 1, 2, 4

63. Simonyan K, Zisserman A (2015) Very deep convolutional networks for large-scale image recognition. In: International Conference on Learning Representations 4

64. Sukhbaatar S, Weston J, Fergus R, et al. (2015) End-to-end memory networks. In: Advances in neural information processing systems, pp 2440–2448 8

65. Sutskever I, Vinyals O, Le QV (2014) Sequence to sequence learning with neural networks. In: Advances in neural information processing systems, pp 3104–3112 4

66. Tai KS, Socher R, Manning CD (2015) Improved semantic representations from tree-structured long short-term memory networks. Proceedings of the 53rd Annual Meeting of the Association for Computational Linguistics and the 7th International Joint Conference on Natural Language Processing of the Asian Federation of Natural Language Processing 3

67. Tang K, Zhang H, Wu B, Luo W, Liu W (2019) Learning to compose dynamic tree structures for visual contexts. In: Proceedings of the IEEE/CVF Conference on Computer Vision and Pattern Recognition, pp 6619–6628 1

68. Toutanova K, Manning CD (2000) Enriching the knowledge sources used in a maximum entropy part-of-speech tagger. In: Proceedings of the 2000 Joint SIGDAT conference on Empirical methods in natural language processing and very large corpora: held in conjunction with the 38th Annual Meeting of the Association for Computational Linguistics-Volume 13, Association for Computational Linguistics, pp 63–70 8

69. Vaswani A, Shazeer N, Parmar N, Uszkoreit J, Jones L, Gomez AN, Kaiser Ł, Polosukhin I (2017) Attention is all you need. In: Advances in Neural Information Processing Systems, pp 5998–6008 1, 4, 6, 7, 14

70. Vedantam R, Lawrence Zitnick C, Parikh D (2015) Cider: Consensus-based image description evaluation. In: Proceedings of the IEEE conference on computer vision and pattern recognition, pp 4566–4575 9, 10

71. Vinyals O, Toshev A, Bengio S, Erhan D (2015) Show and tell: A neural image caption generator. In: CVPR 2, 3

72. Xu B, Wang N, Chen T, Li M (2015) Empirical evaluation of rectified activations in convolutional network. arXiv preprint arXiv:150500853 5

73. Xu D, Zhu Y, Choy CB, Fei-Fei L (2017) Scene graph generation by iterative message passing. In: Proceedings of the IEEE conference on computer vision and pattern recognition, pp 5410–5419 9

74. Xu K, Ba J, Kiros R, Cho K, Courville A, Salakhudinov R, Zemel R, Bengio Y (2015) Show, attend and tell: Neural image caption generation with visual attention. In: International conference on machine learning, pp 2048–2057 3, 4

75. Yang J, Lu J, Lee S, Batra D, Parikh D (2018) Graph r-cnn for scene graph generation. In: Proceedings of the

European conference on computer vision (ECCV), pp 670–685 9

- 76. Yang X, Tang K, Zhang H, Cai J (2019) Auto-encoding scene graphs for image captioning. In: Proceedings of the IEEE Conference on Computer Vision and Pattern Recognition, pp 10685–10694 4, 13, 14
- 77. Yang X, Zhang H, Cai J (2019) Learning to collocate neural modules for image captioning. In: Proceedings of the IEEE International Conference on Computer Vision, pp 4250–4260 3, 7, 10, 13, 14
- 78. Yao T, Pan Y, Li Y, Qiu Z, Mei T (2017) Boosting image captioning with attributes. In: IEEE International Conference on Computer Vision, ICCV, pp 22–29 3, 14
- 79. Yao T, Pan Y, Li Y, Mei T (2018) Exploring visual relationship for image captioning. In: Computer Vision–ECCV 2018, Springer, pp 711–727 4, 13, 14, 15
- 80. Yao T, Pan Y, Li Y, Mei T (2019) Hierarchy parsing for image captioning. In: Proceedings of the IEEE/CVF International Conference on Computer Vision, pp 2621–2629 4, 13, 14, 15
- 81. Yi K, Wu J, Gan C, Torralba A, Kohli P, Tenenbaum J (2018) Neural-symbolic vqa: Disentangling reasoning from vision and language understanding. In: Advances in Neural Information Processing Systems, pp 1031–1042 4
- 82. You Q, Jin H, Wang Z, Fang C, Luo J (2016) Image captioning with semantic attention. In: Proceedings of the IEEE conference on computer vision and pattern recognition, pp 4651–4659 3
- 83. Yu L, Lin Z, Shen X, Yang J, Lu X, Bansal M, Berg TL (2018) Mattnet: Modular attention network for referring expression comprehension. In: Proceedings of the IEEE Conference on Computer Vision and Pattern Recognition, pp 1307–1315 4, 6
- 84. Zellers R, Yatskar M, Thomson S, Choi Y (2018) Neural motifs: Scene graph parsing with global context. In: Proceedings of the IEEE Conference on Computer Vision and Pattern Recognition, pp 5831–5840 6, 9
- 85. Zha ZJ, Liu D, Zhang H, Zhang Y, Wu F (2019) Context-aware visual policy network for fine-grained image captioning. IEEE transactions on pattern analysis and machine intelligence 3, 13, 14
- 86. Zhang H, Kyaw Z, Chang SF, Chua TS (2017) Visual translation embedding network for visual relation detection. In: Proceedings of the IEEE conference on computer vision and pattern recognition, pp 5532–5540 6